

A Compromise Principle in Deep Monocular Depth Estimation

Huan Fu, *Student Member, IEEE*, Mingming Gong, *Student Member, IEEE*, Chaohui Wang *Member, IEEE*,
and Dacheng Tao, *Fellow, IEEE*

Abstract—Monocular depth estimation, which plays a key role in understanding 3D scene geometry, is fundamentally an ill-posed problem. Existing methods based on deep convolutional neural networks (DCNNs) have examined this problem by learning convolutional networks to estimate continuous depth maps from monocular images. However, we find that training a network to predict a high spatial resolution continuous depth map often suffers from poor local solutions. In this paper, we hypothesize that achieving a compromise between spatial and depth resolutions can improve network training. Based on this “compromise principle”, we propose a regression-classification cascaded network (RCCN), which consists of a regression branch predicting a low spatial resolution continuous depth map and a classification branch predicting a high spatial resolution discrete depth map. The two branches form a cascaded structure allowing the classification and regression branches to benefit from each other. By leveraging large-scale raw training datasets and some data augmentation strategies, our network achieves top or state-of-the-art results on the NYU Depth V2[1], KITTI [2], and Make3D [3] benchmarks.

Index Terms—Depth Prediction, Depth Resolution, Spatial Resolution, Compromise Principle, SID, Convolutional Neural Network

I. INTRODUCTION

ESTIMATING depth from 2D images is a key component of scene reconstruction and understanding tasks, such as 3D recognition [4], [3], [5], segmentation [1], [6] and detection [7], *etc.* In this paper, we examine the problem of *Monocular Depth Estimation* (abbr. as *MDE* hereafter), namely the estimation of the depth map from a single image.

Compared to depth estimation from stereo images or video sequences, in which significant progress has been made [8], [9], [10], [11], progress in MDE has been slow. MDE is fundamentally an ill-posed problem: a single 2D image may be produced from an infinite number of distinct 3D scenes. Fortunately, the 2D image and the depth map are correlated, suggesting that the depth can still be predicted with considerable accuracy.

To overcome this inherent ambiguity, typical methods resort to exploiting statistically meaningful monocular cues or features, such as perspective and texture information, object sizes, object locations, and occlusions. Previous methods used

handcrafted features for depth estimation [3], [12], [13], but since the handcrafted features alone can only capture local information, probabilistic graphic models [14], [3] or depth transfer methods [10] have been introduced to incorporate long range global cues.

Buoyed by the success of deep convolutional neural networks (DCNNs) in object recognition and detection, several recent works have significantly improved the MDE performance by a large margin with the use of DCNN-based models [15], [16], [17], [18], [19], [20], demonstrating that deep features are superior to handcrafted features. The main advantage of DCNNs is that the hierarchical representations in a DCNN capture both local and global information. A state-of-the-art method [18] exploits the multi-scale network which firstly learns to predict a coarse depth map using global information and then refines it using another network with local information to produce a fine depth map.

Existing methods address the MDE problem by learning a CNN to estimate the continuous depth map. Since this problem is a standard regression problem, existing methods usually adopt the root mean squared error (RMSE) in log-space as the loss function. Although training with RMSE can achieve a reasonable solution when predicting a low resolution depth map, we find that the optimization tends to be difficult when we try to train networks to predict high-resolution continuous maps. The stochastic gradient descent (SGD) optimization method usually produces a local solution with unsatisfactory training error in this case.

We hypothesize that a compromise between spatial and depth resolution can make the optimization easier, which is referred to as the “compromise principle” in this paper. According to the compromise principle, we avoid directly estimating a high spatial resolution continuous depth map by firstly estimating depth maps with reduced spatial or depth resolution. To reduce the depth resolution, we propose to transform the regression problem into a classification problem by discretizing the depth value into intervals. Employing the classification loss to train the network achieves lower RMSE on the training data than training with RMSE. Also, the low spatial resolution continuous map can be learned with considerable accuracy. Based on such a principle, we develop a regression-classification cascade network (RCCN) which consists of two branches: 1) the regression branch predicting low spatial resolution continuous depth map from the fully-connected layers, capable of capturing global scene information; and 2) the classification branch, which predicts high spatial resolution discrete depth maps from the convolutional

H. Fu and D. Tao are UBTECH Sydney AI Centre, SIT, FEIT, The University of Sydney, J12 Cleveland St, Darlingtown NSW 2008, Australia (e-mail: hufu6371@uni.sydney.edu.au; dacheng.tao@sydney.edu.au).

M. Gong is with CAI, FEIT, University of Technology Sydney, Ultimo, NSW 2007, Australia (e-mail: mingming.gong@student.uts.edu.au).

C. Wang is with Laboratoire d'Informatique Gaspard Monge - CNRS UMR 8049, Université Paris-Est, 77454 Marne-la-Vallée Cedex 2, France (e-mail: chaohui.wang@u-pem.fr).

layers to preserve finer spatial information. The two branches form a cascaded structure and are learned jointly in an end-to-end fashion, which allows the classification and regression branches to benefit from each other. After accomplishing the RCCN learning stage, a refinement and a fusion networks are posted to refine the discrete depth map into a higher spatial resolution. Our network achieves the state-of-the-art performance on NYU Depth V2 [1], KITTI [2], and Make3D [14], [3] benchmarks, which are three challenging datasets commonly used for MDE. In particular, our method outperforms existing methods by a large margin on the two outdoor datasets.

II. RELATED WORK

Depth estimation is an important part of understanding the 3D structure of scenes from 2D images. Most prior works focused on estimating depth from stereo images by developing geometry-based algorithms [21], [22] that rely on point correspondences between images and triangulation to estimate the depth. Given accurate point correspondences, depth can be estimated deterministically from stereo images. Thus, stereo depth estimation has particularly benefitted largely from the advances in local feature matching and dense optical flow estimation techniques.

However, the geometry-based depth estimation algorithms for stereo images ignore the monocular cues in 2D images, which can also be used for depth estimation. In a seminal work [14], Saxena *et al.* learned the depth from monocular cues in 2D images via supervised learning. Since then, a variety of approaches have been proposed to exploit the monocular cues using handcrafted representations [3], [12], [13]. Since handcrafted features alone can only capture local information, probabilistic graphic models such as Markov Random Fields (MRFs) are often built on these features to incorporate long-range and global cues [3], [23], [24]. Another successful way to make use of global cues is the DepthTransfer method [10] which uses GIST global scene features [25] to search for candidate images that are “similar” to the input image from a database containing RGBD images. A warping procedure based on SIFT Flow [26] was then applied to the candidate image and the corresponding depth map to align them to the input image.

Given the success of DCNNs in image understanding [27], [28], [29], [30], some DCNNs based depth prediction frameworks have recently been proposed in recent years [31], [16], [32], [20]. Xie *et al.* [33] predicted the disparity map by adopting multi-level convolutional features for recovering a right view from a left-view. Garg *et al.* [31] proposed an unsupervised framework to learn a deep depth-estimation neural network. Liu *et al.* [15] jointly explored the capacity of DCNNs and continuous CRF in a unified deep structured network. Moreover, Wang *et al.* [16] captured depth values and semantic information in a scene with DCNNs, and integrated them in a two-layer hierarchical CRF to jointly predict depth values and semantic labels. To improve efficiency, Roy and Todorovic [17] proposed the Neural Regression Forest method which allowed for parallelisable training of “shallow” CNNs.

To further incorporate global information in DCNNs, Wang *et al.* [34] proposed a method for surface normal prediction,

where two independent networks were learned to exploit global and local information respectively. Eigen *et al.* [35], [18] proposed a multi-scale network that firstly learned to predict depth at a coarse scale and then refined it using another network to produce fine-scale depth maps. Our RCCN method also explores multi-scale representations in the network for depth prediction. However, our network architecture is motivated by exploiting the compromise between spatial and depth resolutions. Thus, instead of designing a stage-wise refinement procedure as done in [35], we introduce a cascaded structure to learn low spatial resolution but high depth resolution continuous depth via regression and high spatial resolution but low depth resolution discrete depth via classification in an end-to-end fashion. This approach allows the two branches to benefit from each other. In addition, to exploit large receptive field and to alleviate information loss caused by downsampling operation, we introduce dilated convolution [36] to the discrete depth estimation branch. Finally, we employ the deconvolution technique [37] as the bridge between the different branches to balance the feature channels from each branch.

RCCN	layer	b_1	b_2	b_3	r_1	r_2	r_3	r_4	r_5	De	
	convs	2	2	3	3	3	-	-	-	1	
	chans	64	128	256	512	512	2048	2048	1	512	
	kernel	3	3	3	3	3	-	-	-	4	
	dilat	-	-	-	-	-	-	-	-	-	
	ratio	/2	/4	/8	16/	32/	-	-	/16	/8	
	layer	b_1	b_2	b_3	c_1	c_2	Co	c_3	c_4	c_5	De
	convs	2	2	3	3	3	-	1	1	1	1
	chans	64	128	256	512	512	-	2048	2048	M	256
	kernel	3	3	3	3	3	-	3	1	1	4
Refinement	dilat	-	-	-	-	2	-	-	-	-	-
	ratio	/2	/4	/8	/8	/8	/8	/8	/8	/8	/4
	layer	c'_1	c'_2	c'_3			Co	c'_4	c'_5	c'_6	c'_7
	convs	2	2	3			-	1	1	1	1
	chans	64	128	256			-	1024	1024	1024	M
	kernel	3	3	3			-	3	3	1	1
	ratio	/4	/4	/4	/4	/4	/4	/4	/4	/4	/4

TABLE I: **Network Parameters.** Parameters of the proposed network for NYU Depth V2 dataset. b_i : layer shared by the two branches in RCCN. r_i/c_i : layer of the continuous/discrete depth estimation branch. c'_i : layer of the refinement network. Co: concatenation layer. De: deconvolutional layer. M: the number of pre-define sub-intervals.

III. APPROACH

Given an input (indoor or outdoor) image \mathbf{I} of size $H \times W$ (H : height and W : width), we aim to predict its depth map $\mathbf{D} \in \mathbb{R}^{H \times W}$ by exploiting the compromise between spatial and depth resolution. The key component of our approach is the proposed *regression-classification cascaded network* (RCCN). RCCN explicitly models a high spatial resolution discrete depth map \mathbf{D}_1 by discretizing the possible depth interval into a set of discrete values and formulates the estimation of \mathbf{D}_1 as a multi-class classification problem together with the regression of a low spatial resolution continuous depth map \mathbf{D}_0 within the deep architecture. The obtained discrete depth map \mathbf{D}_1 is further refined to obtain a discrete depth map \mathbf{D}_2 in a higher spatial resolution via a refinement network. We describe the detailed architecture of these two networks in Fig. 1 to clearly show their structures and the connections.

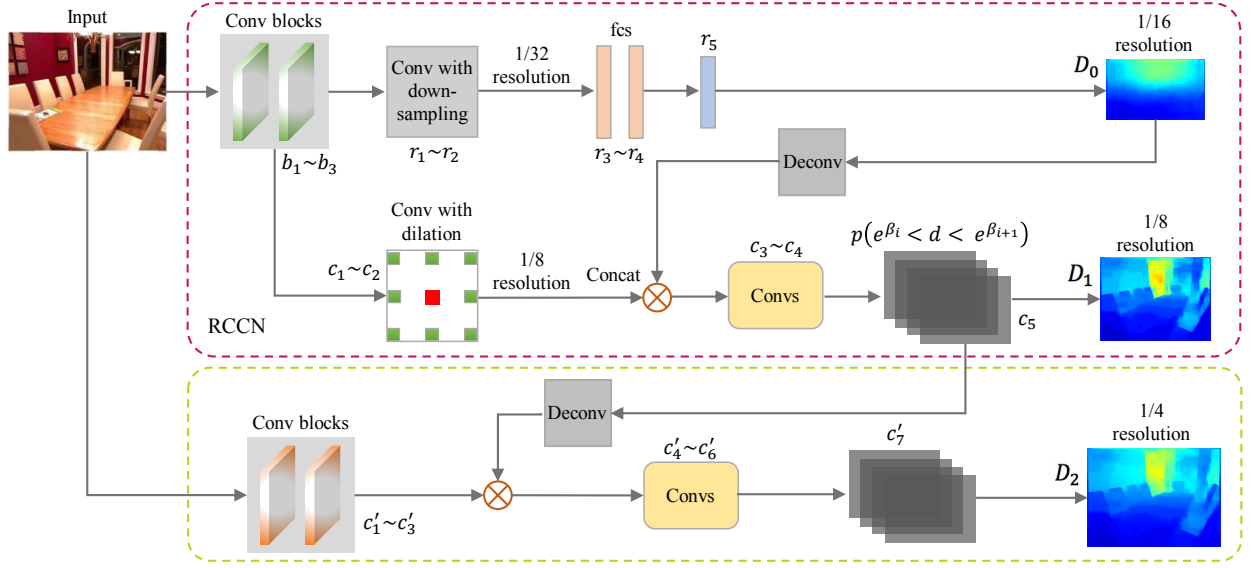


Fig. 1: **Network Architecture** Top: RCCN models the low spatial resolution continuous depth map and the high spatial resolution discrete depth map within a unified network to exploit the compromise between spatial and depth resolution. The regression stage achieves a full-image-view understanding and predicts a low-spatial-resolution continuous depth map. The classification stage takes the low spatial resolution continuous depth map and the convolutional features as inputs, and classifies the pixel at each spatial position to one of the pre-defined discrete depths in a high spatial resolution. Down: The refinement network takes the RGB image and those features from RCCN as inputs, and outputs a discrete depth map in a higher spatial resolution.

Last but not least, the depth maps of all three scales (*i.e.*, D_0 , D_1 , and D_2) can be jointly considered within a fusion network, so as to achieve a continuous depth map \tilde{D}_2^1 . We present the three networks in detail below.²

A. Regression-Classification Cascaded Network

The Regression-Classification Cascaded Network (RCCN) is a joint regressor-classifier. It serves as a two-tier estimator that simultaneously predicts the initial continuous depth map D_0 and the discrete depth map D_1 . We choose to adopt a two-level cascaded network for modeling and implementing the regression-classification network, aiming to exploit the compromise between low spatial resolution continuous depth and high spatial resolution discrete depth. We also incorporate global scene information and local structural and contextual information.

Regressing Continuous Depth: In this stage, the network aims to predict the low spatial resolution continuous depth map D_0 from a global understanding of the entire image, by abstracting a representation feature vector from the whole image field of view. From such a representation, we learn specific non-linear functions for all the pixels located at a pre-defined resolution ($h \times w$).

To this end, on top of the shared convolutional layers (b_1 to b_3), additional convolutional layers (r_1 and r_2) and max-pooling layers with downsampling are used to obtain deeper convolutional features at a coarse resolution. Then, after the pass of two fully-connected (fc) layers (r_3 and r_4), the feature vector will contain high-level information of the whole input image. Followed by a third fc layer (r_5) with $h \times w$ outputs, each output represents the depth value of a spatial location within the pre-defined resolution, and connects to all the vector elements from the last layer, implying a global understanding of the entire image.

This stage is supervised by manually labeled continuous depth values over the whole input image via root mean squared error in log space ($RMSE_{log}$). More specifically, we reshape the hw -dimensional output vector to a $h \times w$ map, and up-sample it to the original resolution ($H \times W$) to obtain the predicted depth map D' at this stage to compare it with the target depth map D^* . The loss term $Loss_1$ takes the following form:

$$Loss_1 = Loss_1(D', D^*) = \sqrt{\frac{1}{N - N'} \sum_{i=1}^N \theta_i \|\log(d'_i) - \log(d_i^*)\|^2}, \quad (1)$$

where $N = H \times W$ is the total number of pixels in the input image, and $d'_i \in D'$ and d_i^* denotes the predicted and ground truth depths of pixel i , respectively. In this stage, d'_i and d_i^* are real continuous values. Considering the fact that the target depth map D^* may have missing values, the back propagation in our network only relies on valid pixels (*i.e.*, pixels with depth values). Thus, in Eq. 1, θ_i equals to 1 when pixel i has

¹In practice, if the resolution of the depth map output by the deep model is lower than $H \times W$, a classic interpolation method (*e.g.*, linear interpolation) can be used to obtain the depth map at full resolution.

²We introduce our approach based on the network setting for our experiment on NYU Depth V2 dataset and Tab. I provides the associated parameters, so as to facilitate the understanding of the whole approach. The network setting and parameters can be replaced by other appropriate ones.

a valid depth value, otherwise 0, and N' denotes the number of pixels with missing depth values.

It should be noted that, the $RMSE_{log}$ loss uses a log function to down-weight the losses in regions with large depth values, which is commonly used as an evaluation metric. From a statistical view, let us consider the generation of data following $y = \exp(\log(x) + N(0, 1))$ with x uniform distributed. It is easy to observe that the noise variance of y is larger when x is larger, implying that the observed depth value has a larger noise variance when its ground truth is larger. Hence, without log , large depth values would induce an over-strengthened influence on the training process, which is not expected. It also motivates the SID method (instead of uniform quantization) for classification as below, which quantizes depth values with increasing intervals and whose advantage is quantitatively evaluated.

Categorizing Approximate Depth: This stage categorizes each pixel to one of the pre-defined discrete depths in a higher spatial resolution, by taking the shared convolutional features and the previous-stage depth map as inputs.

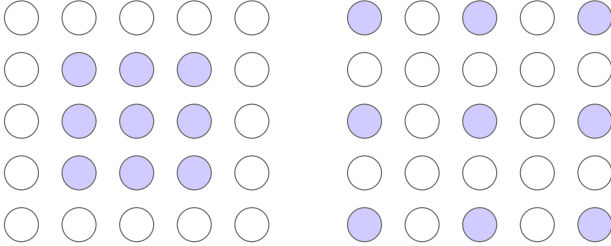


Fig. 2: **Dilated Convolution.** Red/green circle: input/output. Top: regular convolutional layer (c_1). Bottom: dilated convolutional layer (c_2).

Specifically, in order to better exploit the compromise between spatial and depth resolution as well as the geometric contexts and physical properties of the image, we adopt a cascaded structure in which the previous-stage depth map is fed into the classification network. The previous-stage depth map is spatially coarse (low spatial resolution) but provides a global-field-of-view understanding of the input image. The shared convolutional features contain finer spatial information. Therefore, on top of the shared convolutional layers, additional convolutional layers (c_1 and c_2) are used to obtain local structural and contextual information. In contrast to the regression branch, we skip the subsampling operation in the max-pooling layers and employ the dilated convolution technique (c_2) [36], which introduces zeros to increase the convolution field to exploit large receptive field information in the fine resolution feature map, as shown in Fig. 2. The predicted continuous depth map is simultaneously deconvoluted to multi-channel feature maps with the same spatial resolution as c_2 . The deconvolution to multi-channel features is an important component to balance the features from different branches. Followed by a concatenation layer, three extra convolutional layers (c_3 to c_5) are applied to learn a richer representation and model the probabilities of the depth sub-intervals that each pixel belongs

to.

This stage is supervised by the pre-defined discrete depths like semantic labels in segmentation tasks. We minimize the multinomial logistic loss to learn the network parameters. The loss term $Loss_2$ takes the following form:

$$Loss_2 = Loss_2(D'', D^*) \\ = \frac{-1}{N - N'} \sum_{i=1}^N \theta_i \sum_{j=0}^M \delta(l_j < d_i^* \leq l_{j+1}) \log(P''_{ij}), \quad (2)$$

where $P''_{ij} = P(l_j < d_i'' \leq l_{j+1})$ denotes the probability via softmax function, and $\delta(\cdot)$ an indicator function ($\delta(True) = 1$ and $\delta(False) = 0$). The real numbers l_0 to l_M ($l_0 < l_1 < \dots < l_M$) are scale values that discretize the depth interval to M sub-intervals.

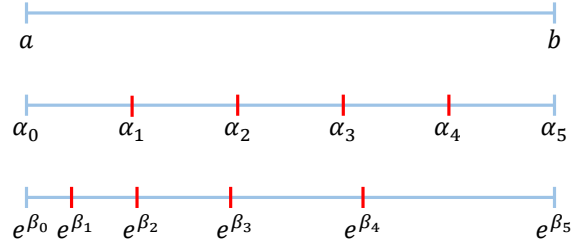


Fig. 3: **Discrete Intervals.** An illustration of UD (middle) and SID (bottom) to discrete depth interval $[a, b]$ into five sub-intervals. See Eq. 3 for detail.

Uniform discretization (UD) is a common way to obtain a set of representative values from a depth interval $[a, b]$. However, considering the facts that it is more difficult for the humans to tell whether an object is 10m or 11m away than 1m or 2m away, and that the importance of a fixed interval (e.g., 0.5m) decreases when the depth ranges from small to large, we propose to use the following spacing-increasing discretization (SID) strategy (as shown in Fig. 3) so that the learned model pays more attention to estimating relatively small depths:

$$\begin{aligned} \text{UD: } l_j &= a + (b - a) * j / M \\ \text{SID: } l_j &= e^{\log(a) + \frac{\log(b/a) * j}{M}} \end{aligned} \quad (3)$$

In contrast to traditional multi-task learning, the latter loss term in the cascade framework relies on the outputs of the former one. The chain rule is applied to seek gradients of $Loss_1 + Loss_2$, and back-propagation is used to perform end-to-end training.

B. Refinement Network

By taking the input RGB image and the features of the last classification branches of RCCN as inputs, the refinement network incorporate multi-scale features (implying different receptive field sizes) and refines the discrete depth map into a higher spatial resolution.

Via those convolution blocks (c'_1 to c'_3), we obtain features at a 1/4 resolution of the original image (a relative small receptive field). Similar to the second stage in RCCN, the features (c'_5) are deconvoluted into the same resolution of c'_3

with multi-channels outputs. Then, convolutional layers (c'_4 to c'_8) are applied on these two scales of features to obtain the refined discrete depth map. The supervised information in this refinement network is the same as the one in the second stage of RCCN, except for the higher spatial resolution. We initialize the trained parameters of $c'_1 \sim c'_3$ using those of $b_1 \sim b_3$ in our experiments³.

C. Fusion Network

The depth map from the refinement network already incorporates multi-scale features in multi-scale receptive fields, and on average achieves a more accurate depth map estimation than those two predicted maps of RCCN, but not for all individual pixels. There are two possible reasons for such a phenomenon: (i) the refined depth map is still in discrete space; or (ii) depth estimation for some objects (especially for large objects) depends more on information from large receptive fields, and features from small receptive fields may introduce some noises. To address this, we integrate the depth maps from all three scales within the fusion network, which just consists of a few convolutional layers in our experiments. Also, the supervised information in the fusion network is the same as that in the first stage of RCCN except for the higher spatial resolution.

IV. EXPERIMENTS

To validate the compromise principle and demonstrate the effectiveness of RCCN, here we present a number of experiments examining different aspects of the approach. After introducing the common experimental settings, we evaluate our methods on three challenging datasets, *i.e.* *NYU Depth V2* [1], *KITTI* [2], and *Make3D* [14], [3], via the error metrics using in previous works.

A. Experimental Setting

Implementation In order to fairly compare the proposed method with the current state-of-the-art methods [18], our method adopts the 16-layer VGG [39] as our base convolutional architecture instead of the more powerful ResNet [40]. We initialise the VGG16 parameters via the pre-trained classification model on ILSVRC [41]. We firstly learn RCCN in an end-to-end fashion. The learning strategy for RCCN follows a polynomial decay with a base learning rate of 0.0002, the power of 0.9, the momentum of 0.9, and the weight decay of 0.0005. Further, we train the higher scale refinement network independently by fixing the parameters and following the same solver script in RCCN. Finally, we fix the parameters in the whole network architecture and learn the fusion network with the starting learning rate of 0.0001. The proposed algorithm is implemented in *Caffe* [42], and trained on 4 TITAN X GPUs with 12GB of memory per GPU.

Data Augmentation Following previous works [35], [38], we employ some data augmentation techniques to prevent overfitting and to learn a better model in the training

process, including: (i) *Random Cropping*: we randomly crop rectangles with predefined sizes from the original image. (ii) *Flipping*: we randomly flip the original image horizontally. (iii) *Scaling*: we randomly resize the original image by a scale factor belongs to the interval of $[1.0, 1.4]$, and normalize the associated depth map with the corresponding scales. (iv) *Rotation*: we randomly rotate the input image with the degree of $[-10^\circ, 10^\circ]$.

Error Metrics: Below are the list of depth error metrics based on which the quantitative evaluation is performed:

PCT- δ : the percentage of pixels satisfying $\max(\frac{d_i}{d_i^*}, \frac{d_i^*}{d_i}) < \delta$

$$\begin{aligned}
 \text{Abs Rel Diff: } & \frac{1}{N} \sum_{i \in N} \frac{|d_i - d_i^*|}{d_i^*} \\
 \text{Squa Rel Diff: } & \frac{1}{N} \sum_{i \in N} \left(\frac{d_i - d_i^*}{d_i^*} \right)^2 \\
 \text{RMSE-linear: } & \sqrt{\frac{1}{N} \sum_{i \in N} \|d_i - d_i^*\|^2} \\
 \text{RMSE-log: } & \sqrt{\frac{1}{N} \sum_{i \in N} \|\log(d_i) - \log(d_i^*)\|^2} \\
 \text{Ave log}_{10} \text{ Error: } & \frac{1}{N} \sum_{i \in N} |\log_{10}(d_i) - \log_{10}(d_i^*)|
 \end{aligned} \tag{4}$$

B. KITTI

The KITTI dataset [2] contains some outdoor scenes captured by cameras and depth sensors in a driving car. All the 61 scenes from the “city”, “residential”, and “road” categories consist of our training/test sets. We test on 697 images from 28 scenes split by [35], and train on 23,486 images from the remaining 33 scenes. We train our model on a random crop of size 288×384 . Since the ground truth depth are provided for only about 15% of points within the bottom part of the image, some depth targets in the bottom parts are filled using the colorization routine in the NYU Depth development kit [43] for our training images following [35]. Besides those representative quantitative results shown in Fig. 4, we summarize the quantitative evaluation in Tab. II, which demonstrates that the proposed approach significantly outperforms those previous methods in all those considered error metrics.

Furthermore, in order to evaluate the importance of the depth interval discretization, we have compared the performance of RCCN with one variant (referred to as *RCCN-UD*) which uses the UD discretization strategy instead of SID, and the results shown in Tab. II demonstrate that both *RCCN-UD* and *RCCN-SID* achieve very good performance and the use of SID strategy improves further the performance.

To further exploit the compromise principle and demonstrate the effectiveness of the proposed RCCN, we learn some related network variants by directly regressing continuous depth, directly estimating discrete depth via classification, jointly modeling continuous depth via our network architecture, and

³Note that $c'_1 \sim c'_3$ are independent from $b_1 \sim b_3$.

Algorithm	Metric						
	higher is better			lower is better			
	$\delta < 1.25$	$\delta < 1.25^2$	$\delta < 1.25^3$	abs rel diff	squa rel diff	RMSE _{linear}	RMSE _{log}
Make3D [3]	0.601	0.820	0.926	0.280	3.012	8.734	0.361
Eigen <i>et al.</i> [35]	0.692	0.899	0.967	0.190	1.515	7.156	0.270
Liu <i>et al.</i> [15]	0.647	0.882	0.961	0.217	1.841	6.986	0.289
Garg <i>et al.</i> [31]	0.740	0.904	0.962	0.169	1.080	5.104	0.273
Godard <i>et al.</i> [32]	0.818	0.929	0.966	0.141	1.369	5.849	0.242
Kuznetsov <i>et al.</i> -ResNet [20]	0.848	0.958	0.986	0.123	0.859	4.903	0.194
RCCN-UD	0.780	0.930	0.975	0.158	1.038	5.321	0.228
RCCN-SID	0.852	0.963	0.990	0.123	0.763	4.235	0.174
RCCN-Refine	0.870	0.970	0.993	0.110	0.620	4.029	0.160
RCCN-Refine-Fusion	0.886	0.975	0.994	0.105	0.540	3.903	0.154

TABLE II: **Performance on KITTI test set.** RCCN-UD: RCCN whose discrete depth branch is supervised by uniform discretised sub-intervals. RCCN-SID: RCCN whose discrete depth branch is supervised by spacing-increase discretised sub-intervals. RCCN-Refine: RCCN-SID with refinement network. RCCN-Refine-Fusion: RCCN-SID with refinement network and fusion network.

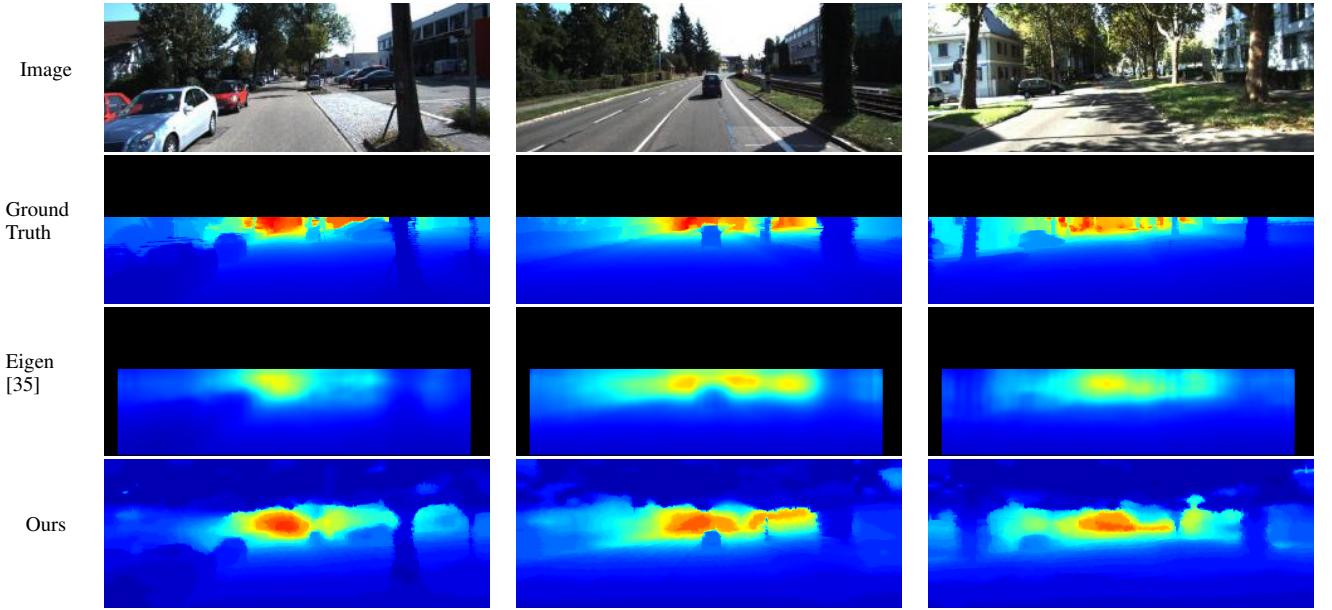


Fig. 4: **KITTI Results.** Image, ground truth, Eigen [35], and Our result. (Best view in color.)

learning a classification-classification cascade network. From the quantitative results shown in Tab. IV and Fig. 6, we can conclude that: 1) when treating depth estimation as a classification problem instead of regression, the network can converge to a better local solution on average; 2) image-receptive-field-of-view understanding, as well as local high-level convolutional features indeed help deep networks better learn the depth distribution of a scene; 3) the compromise between spatial and depth resolutions simplifies network training; 4) The performances of RCCN and of RCCN deteriorate once removing the low-spatial resolution branch D_0 from them (leading to R, C, respectively), demonstrating that D_0 benefits D_1 ; 5) The comparison between D_0 and RCCN- D_0 shows that D_1 also benefits D_0 ; and 6) From the observation that $\text{RCCN} > \text{CCCN} > \text{RRCN}$, It can be seen that high spatial resolution together with high depth resolution leads to worse results.

C. NYU Depth V2

The NYU Depth V2 [1] contains 464 indoor video scenes taken with a Microsoft Kinect camera. We randomly sample half of the 120K images from the raw dataset according to the official split training scenes as our training sets, and test on the 694-image test set. We train our model on a randomly crop of size 240×320 . On top of those qualitative results in Fig. 5, we report in Tab. III the quantitative results via several common metrics used in previous works [18], [15]. The predictions from our model yields comparable or state-of-the-art results comparison with previous works. Specifically, the estimated coarse continuous depth outperforms the “Coarse+Fine” prediction of Eigen *et al.* [35]. The predicted high spatial resolution discrete depth in particular obtains an impressive improvement, demonstrating that both discrete depth and the proposed RCCN framework are effective.

Algorithm	Metric						
	higher is better			lower is better			
	$\delta < 1.25$	$\delta < 1.25^2$	$\delta < 1.25^3$	abs rel diff	squa rel diff	RMSE _{linear}	RMSE _{log}
Make3D [3]	0.447	0.745	0.897	0.349	0.492	1.214	0.409
DepthTransfer [10]	-	-	-	0.350	-	1.2	-
Ladicky <i>et al.</i> [13]	0.542	0.829	0.941	-	-	-	-
Liu <i>et al.</i> [15]	0.614	0.883	0.971	0.230	-	0.824	-
Wang <i>et al.</i> [16]	0.605	0.890	0.970	0.220	0.210	0.745	0.262
Roy <i>et al.</i> [17]	-	-	-	0.187	-	0.744	-
Laina <i>et al.</i> -VGG [38]	0.629	0.889	0.971	0.215	-	0.790	-
Eigen-Coarse+Fine [35]	0.611	0.887	0.971	0.215	0.212	0.907	0.285
RCCN-UD	0.733	0.930	0.980	0.178	0.158	0.628	0.223
RCCN-SID	0.747	0.928	0.978	0.175	0.157	0.630	0.226
Eigen-Refinement [18]	0.769	0.950	0.988	0.158	0.121	0.641	0.214
RCCN-Refine	0.753	0.937	0.983	0.165	0.138	0.607	0.213
RCCN-Refine-Fusion	0.765	0.950	0.991	0.160	0.131	0.586	0.204

TABLE III: **Performance on NYU Depth V2 test set.** RCCN-UD: RCCN whose discrete depth branch is supervised by uniform discretised sub-intervals. RCCN-SID: RCCN whose discrete depth branch is supervised by spacing-increase discretised sub-intervals. RCCN-Refine: RCCN-SID with refinement network. RCCN-Refine-Fusion: RCCN-SID with refinement network and fusion network.

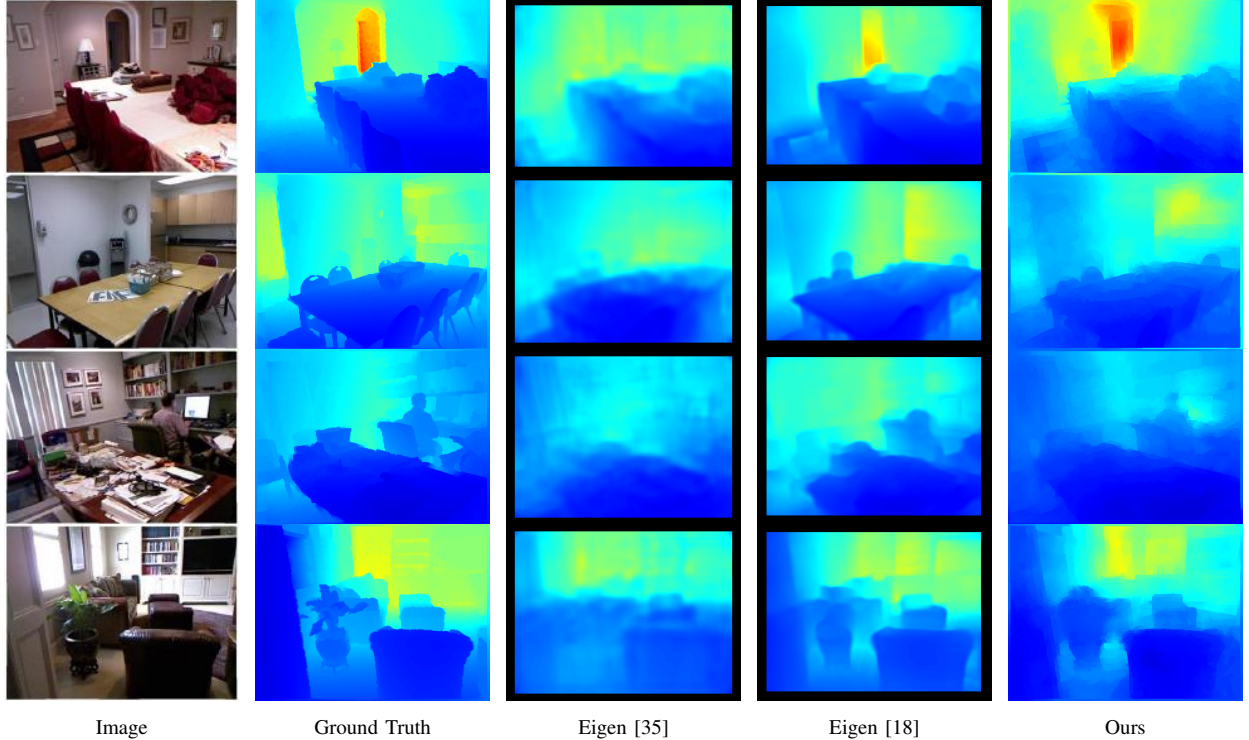


Fig. 5: **NYU Depth V2 Results.** Image, ground truth, Eigen [35], Eigen [18], and Our result. (Best view in color.)

D. Make3D

The Make3D dataset [14], [3] contains 534 outdoor images, 400 for training, and 134 for testing, with the resolution of 2272×1704 . Our model is trained on a random crop of size 480×320 . In the test phase, we split the test images into some 480×320 sub-images, and use max pooling on the overlapping regions to obtain the final predictions. As shown in Tab. V, we report $C1$ and $C2$ error on this dataset [10]. We achieve state-of-the-art performance in all error metrics.

V. CONCLUSION

In this paper, we have presented a deep CNN architecture for MDE. Based on the fact that training a network to estimate a high spatial resolution continuous depth map is difficult, we hypothesize to design network architectures according to the compromise principle that training a network to estimate a depth map with reduced spatial resolution or depth resolution is easier. According to the compromise principle, we propose a regression-classification cascaded network to jointly model continuous depth and discrete depths in two branches. The

	R	C	RRCN	RCCN	CCCN	D_0	RCCN- D_0
$\delta < 1.25$	0.732	0.806	0.762	0.852	0.835	0.741	0.750
$\delta < 1.25^2$	0.905	0.947	0.928	0.963	0.950	0.913	0.919
$\delta < 1.25^3$	0.951	0.985	0.968	0.990	0.982	0.956	0.960
abs rel diff	0.172	0.142	0.162	0.123	0.132	0.168	0.162
squa rel diff	1.105	0.892	1.060	0.763	0.893	1.092	1.071
RMSE _{linear}	5.829	4.711	5.105	4.235	5.102	5.476	5.265
RMSE _{log}	0.282	0.198	0.235	0.174	0.208	0.270	0.247

TABLE IV: **Variants of RCCN on KITTI dataset.** R: Directly learning continuous depth in a fine scale via regression. C: Directly learning discrete depth in a fine scale via classification with proposed SID strategy. RRCN: Learning continuous depth via a cascaded regression-regression structure. RCCN: The proposed method. CCCN: A classification-classification cascade network. Note that, higher is better in top table, while lower is better in bottom table.

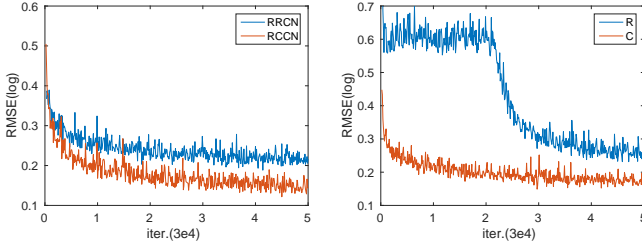


Fig. 6: **Training Error on KITTI dataset.** Left: Training errors of RRCN and RCCN. Right: Training error of R and C. From the two illustrations, our classification strategy (C) for depth estimation can make the neural network converge to a better solution rather than regression strategy (R).

Algorithm	C2 error			C1 error		
	rel	log ₁₀	rms	rel	log ₁₀	rms
Make3D [3]	0.370	-	0.187	-	-	-
Liu <i>et al.</i> [44]	0.375	-	0.148	-	-	-
DepthTransfer [10]	0.361	15.10	0.148	0.355	9.20	0.127
Liu <i>et al.</i> [24]	0.338	12.60	0.134	0.335	9.49	0.137
Liu <i>et al.</i> [15]	0.307	12.89	0.125	0.314	8.60	0.119
Roy <i>et al.</i> [17]	0.26	12.40	0.119	-	-	-
Ours	0.255	11.57	0.106	0.252	6.68	0.081

TABLE V: **Performance on Make3D test set.**

regression and classification branches benefit from each other due to the cascaded structure and joint end-to-end training. The proposed approach is validated on three widely-used and challenging datasets, where it achieves top or state-of-the-art results. Moreover, specific experiments have been done and the obtained results demonstrate that our network is superior to its variants, which also validates the design of our approach to some extent. We will continue to investigate new methodologies to reduce the depth resolution and extend our framework to other challenging dense prediction problems.

REFERENCES

- [1] P. K. Nathan Silberman, Derek Hoiem and R. Fergus, “Indoor segmentation and support inference from rgb-d images,” in *ECCV*, 2012.
- [2] A. Geiger, P. Lenz, C. Stiller, and R. Urtasun, “Vision meets robotics: The kitti dataset,” *IJPR*, 2013.
- [3] A. Saxena, M. Sun, and A. Y. Ng, “Make3d: Learning 3d scene structure from a single still image,” *IEEE TPAMI*, vol. 31, no. 5, pp. 824–840, 2009.
- [4] D. Hoiem, A. A. Efros, and M. Hebert, “Automatic photo pop-up,” *ACM TOG*, vol. 24, no. 3, pp. 577–584, 2005.
- [5] Y. Kong, B. Satarboroujeni, and Y. Fu, “Learning hierarchical 3d kernel descriptors for rgb-d action recognition,” *CVIU*, vol. 144, pp. 14–23, 2016.
- [6] D. Sun, E. B. Sudderth, and M. J. Black, “Layered image motion with explicit occlusions, temporal consistency, and depth ordering,” in *NIPS*, 2010.
- [7] S. Savarese and L. Fei-Fei, “3d generic object categorization, localization and pose estimation,” in *ICCV*, 2007.
- [8] H. Ha, S. Im, J. Park, H.-G. Jeon, and I. S. Kweon, “High-quality depth from uncalibrated small motion clip,” in *CVPR*, 2016.
- [9] N. Kong and M. J. Black, “Intrinsic depth: Improving depth transfer with intrinsic images,” in *ICCV*, 2015.
- [10] K. Karsch, C. Liu, and S. B. Kang, “Depth transfer: Depth extraction from video using non-parametric sampling,” *IEEE TPAMI*, vol. 36, no. 11, pp. 2144–2158, 2014.
- [11] A. Rajagopalan, S. Chaudhuri, and U. Mudenagudi, “Depth estimation and image restoration using defocused stereo pairs,” *IEEE TPAMI*, vol. 26, no. 11, pp. 1521–1525, 2004.
- [12] D. Hoiem, A. A. Efros, and M. Hebert, “Recovering surface layout from an image,” *IJCV*, vol. 75, no. 1, pp. 151–172, 2007.
- [13] L. Ladicky, J. Shi, and M. Pollefeys, “Pulling things out of perspective,” in *CVPR*, 2014.
- [14] A. Saxena, S. H. Chung, and A. Y. Ng, “Learning depth from single monocular images,” in *NIPS*, 2005.
- [15] F. Liu, C. Shen, and G. Lin, “Deep convolutional neural fields for depth estimation from a single image,” in *CVPR*, 2015.
- [16] P. Wang, X. Shen, Z. Lin, S. Cohen, B. Price, and A. Yuille, “Towards unified depth and semantic prediction from a single image,” in *CVPR*, 2015.
- [17] A. Roy and S. Todorovic, “Monocular depth estimation using neural regression forest,” in *CVPR*, 2016.
- [18] D. Eigen and R. Fergus, “Predicting depth, surface normals and semantic labels with a common multi-scale convolutional architecture,” in *ICCV*, 2015.
- [19] S. Kim, K. Park, K. Sohn, and S. Lin, “Unified depth prediction and intrinsic image decomposition from a single image via joint convolutional neural fields,” in *ECCV*, 2016.
- [20] Y. Kuznetsov, J. Stückler, and B. Leibe, “Semi-supervised deep learning for monocular depth map prediction,” in *CVPR*, 2017.
- [21] D. Scharstein and R. Szeliski, “A taxonomy and evaluation of dense two-frame stereo correspondence algorithms,” *IJCV*, vol. 47, no. 1-3, pp. 7–42, 2002.
- [22] D. Forsyth and J. Ponce, *Computer Vision: a Modern Approach*. Prentice Hall, 2002.
- [23] W. Zhuo, M. Salzmann, X. He, and M. Liu, “Indoor scene structure analysis for single image depth estimation,” in *CVPR*, 2015.
- [24] M. Liu, M. Salzmann, and X. He, “Discrete-continuous depth estimation from a single image,” in *CVPR*, 2014.
- [25] A. Oliva and A. Torralba, “Modeling the shape of the scene: A holistic representation of the spatial envelope,” *IJCV*, vol. 42, no. 3, pp. 145–175, 2001.
- [26] C. Liu, J. Yuen, and A. Torralba, “Sift flow: Dense correspondence across scenes and its applications,” *IEEE TPAMI*, vol. 33, no. 5, pp. 978–994, 2011.
- [27] J. Dai, K. He, and J. Sun, “Instance-aware semantic segmentation via multi-task network cascades,” in *CVPR*, 2016.

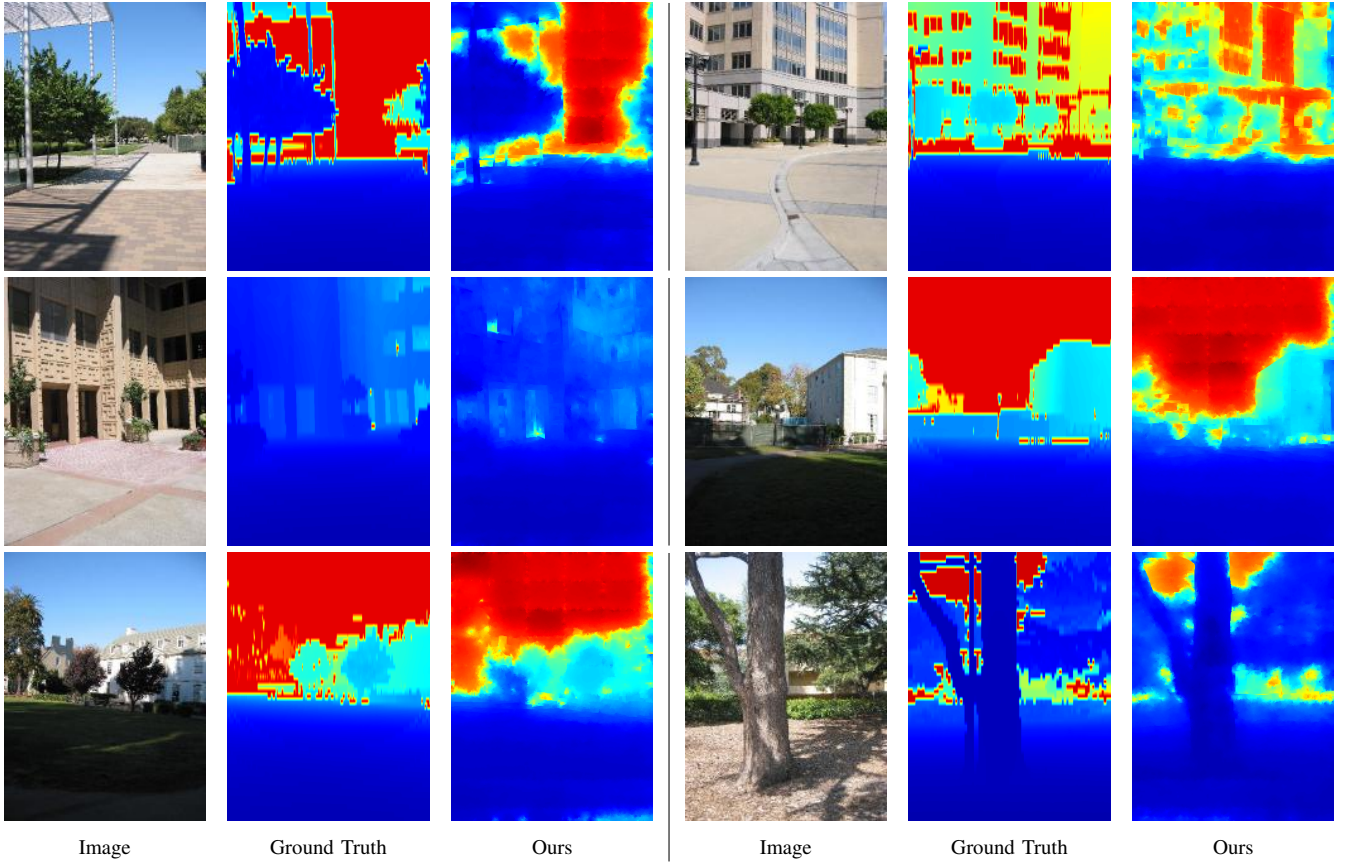


Fig. 7: **Make3D Results.** Image, ground truth, and our results. (best view in color)

- [28] C. Szegedy, S. Ioffe, and V. Vanhoucke, “Inception-v4, inception-resnet and the impact of residual connections on learning,” *arXiv preprint arXiv:1602.07261*, 2016.
- [29] Y. Sun, X. Wang, and X. Tang, “Deep convolutional network cascade for facial point detection,” in *CVPR*, 2013.
- [30] G.-J. Qi, “Hierarchically gated deep networks for semantic segmentation,” in *CVPR*, 2016.
- [31] R. Garg, B. V. Kumar, G. Carneiro, and I. Reid, “Unsupervised cnn for single view depth estimation: Geometry to the rescue,” in *ECCV*, 2016.
- [32] C. Godard, O. Mac Aodha, and G. J. Brostow, “Unsupervised monocular depth estimation with left-right consistency,” *arXiv preprint arXiv:1609.03677*, 2016.
- [33] J. Xie, R. Girshick, and A. Farhadi, “Deep3d: Fully automatic 2d-to-3d video conversion with deep convolutional neural networks,” in *ECCV*, 2016.
- [34] X. Wang, D. Fouhey, and A. Gupta, “Designing deep networks for surface normal estimation,” in *CVPR*, 2015.
- [35] D. Eigen, C. Puhrsch, and R. Fergus, “Depth map prediction from a single image using a multi-scale deep network,” in *NIPS*, 2014.
- [36] L.-C. Chen, G. Papandreou, I. Kokkinos, K. Murphy, and A. L. Yuille, “Deeplab: Semantic image segmentation with deep convolutional nets, atrous convolution, and fully connected crfs,” *arXiv:1606.00915*, 2016.
- [37] M. D. Zeiler, D. Krishnan, G. W. Taylor, and R. Fergus, “Deconvolutional networks,” in *CVPR*, 2010.
- [38] I. Laina, C. Rupprecht, V. Belagiannis, F. Tombari, and N. Navab, “Deeper depth prediction with fully convolutional residual networks,” in *3DV*, 2016.
- [39] K. Simonyan and A. Zisserman, “Very deep convolutional networks for large-scale image recognition,” in *ICLR*, 2015.
- [40] K. He, X. Zhang, S. Ren, and J. Sun, “Deep residual learning for image recognition,” in *CVPR*, 2016.
- [41] O. Russakovsky, J. Deng, H. Su, J. Krause, S. Satheesh, S. Ma, Z. Huang, A. Karpathy, A. Khosla, M. Bernstein, A. C. Berg, and L. Fei-Fei, “ImageNet Large Scale Visual Recognition Challenge,” *IJCV*, vol. 115, no. 3, pp. 211–252, 2015.
- [42] Y. Jia, E. Shelhamer, J. Donahue, S. Karayev, J. Long, R. Girshick, S. Guadarrama, and T. Darrell, “Caffe: Convolutional architecture for fast feature embedding,” *arXiv preprint arXiv:1408.5093*, 2014.
- [43] A. Levin, D. Lischinski, and Y. Weiss, “Colorization using optimization,” *ACM TOG*, vol. 23, no. 3, pp. 689–694, 2004.
- [44] B. Liu, S. Gould, and D. Koller, “Single image depth estimation from predicted semantic labels,” in *CVPR*, 2010.